Biosensors and Bioelectronics 47 (2013) 199–205

Contents lists available at SciVerse ScienceDirect

Biosensors and Bioelectronics

journal homepage: www.elsevier.com/locate/bios

Discrimination of enantiomers based on LSPR biosensors fabricated with weak enantioselective and nonselective receptors

Longhua Guo [a,*], Daifang Wang [a], Yang Xu [a], Bin Qiu [a], Zhenyu Lin [a], Hong Dai [b], Huang-Hao Yang [a], Guonan Chen [a,**]

[a] Ministry of Education Key Laboratory of Analysis and Detection Technology for Food Safety (Fuzhou University), Fujian Provincial Key Laboratory of Analysis and Detection Technology for Food Safety, Department of Chemistry, Fuzhou University, Fuzhou 350108, China
[b] College of Chemistry and Chemical engineering, Fujian Normal University, Fuzhou, Fujian 350108, China

ARTICLE INFO

Article history:
Received 22 November 2012
Received in revised form
3 March 2013
Accepted 4 March 2013
Available online 21 March 2013

Keywords:
Chiral separation
Chiral drug
Enantioselective sensors
LSPR

ABSTRACT

Chiral recognition based on enantioselective sensors is superior to conventional chromatographic enantioseparation techniques in terms of simplicity and rapidity. Normally, highly specific enantioselective receptors are used for the fabrication of enantioselective sensors. However, to date there only limited number of highly specific chiral selectors are reported, which greatly confines the development of enantioselective sensors. Herein, we demonstrate the feasibility of using relatively weak chiral selectors to construct an enantioselective biosensor for accurate chiral discrimination of enantiomers. The detection of racemic mixture of (*R*)- and (*S*)-1,2,3,4-Tetrahydro-1-naphthylamine (TNA) was demonstrated as an example. The sensor was made up of a dual-channel microfluidic chip. One channel of the chip was modified with human serum albumin (HSA), which was reported to be a weak chiral selector for TNA; while the other channel was modified with a monoclonal anti-TNA antibody, which was a non-enantioselective TNA receptor. A portable localized surface plasmon resonance (LSPR) detection system was integrated with the microfluidic chip to accomplish the signal collection. Our investigation revealed that the combination of LSPR responses obtained from the two channels can be used for quantitative discrimination of the (*R*)- and (*S*)-TNA. The limit of detection was found to be 150 nM for (*R*)-TNA and 100 nM for (*S*)-TNA. The feasibility of use relatively weak chiral selectors could potentially promote the development of various enantioselective sensors.

1. Introduction

The impact of chiral compounds on pharmacological processes has been well recognized (Ikai and Okamoto, 2009; Ward and Ward, 2012). It is reported that the worldwide sales of single-enantiomer-dosage drugs is growing at about 13% annual rates over past few years. E.g., among the top ten drugs in sale in the year of 2010 in US, eight are chiral drugs (Wu and Vogt, 2012). It is undoubtedly that the pharmaceutical industry will continue to bring more single-enantiomer drugs to market in lieu of racemic mixtures.

In response to the rising industrial demand of enantiomerically pure drugs, it is essential to develop analytical approaches for quantitative discrimination of single stereoisomers in samples to support both drug development and pharmaceutical quality control. Hitherto, chromatography and electrophoresis based chiral discrimination are the most common techniques used for the analysis of chiral drugs (Ward and Ward, 2012). The major advantage of these approaches lies in the use of weak chiral selectors for separation. This enables the use of a large variety of compounds for molecular recognition of enantiomers: e.g., crown ethers, (Bako et al., 2012; Hirose et al., 2012) natural polysaccharides, (Shen et al., 2010, 2012) cyclodextrins, (Sohajda et al., 2012; Song and Bai, 2009; Zhou et al., 2012) polyether antibiotics, (Guo et al., 2012b; Tang et al., 2012) macro cyclic antibiotics, (Ema et al., 2010; Sun et al., 2009; Ward and Baker, 2008) and maltodextrins (Nojavan and Fakhari, 2011; Płotka et al., 2012; Stefan-van Staden et al., 2011) have been reported for enantioselective discrimination of chiral drugs. In the past few years, our group also concentrated on the development of capillary electrophoresis (CE), (Huang et al., 2007, 2008, 2009; Ye et al., 2010) capillary electrochromatography (CEC) (Huang and Chen, 2011; Lu et al., 2008) and micellar electrokinetic chromatography (MEKC) (Lin et al., 2010; Yu et al., 2012) based approaches for chiral analysis. It should be noted that all the chromatography and electrophoresis based assays involve two steps, namely, the separation and the detection steps, for chiral discrimination. Therefore, the major limitation of these approaches lies in the time-consuming analytical process.

Recently, enantioselective sensors are immersing as a good alternative to conventional chromatography based approaches to be used for the analysis of chiral compounds. One of the

* Corresponding author. Tel.: +86 591 22866164; fax: +86 591 22866135.
** Corresponding author. Tel.: +86 591 22866132; fax: +86 591 22866135.
E-mail addresses: guolh@fzu.edu.cn (L. Guo), gnchen@fzu.edu.cn (G. Chen).

0956-5663/$ - see front matter Crown Copyright © 2013 Published by Elsevier B.V. All rights reserved.
http://dx.doi.org/10.1016/j.bios.2013.03.009

predominant advantages of enantioselective sensors is no separation steps are required (Izake, 2007). Consequently, chiral discrimination based on enantioselective sensors is rapid, and the equipment is relatively simple. In recent years people have developed colorimetric (Cho et al., 2011; Zhang and Ye, 2011; Zhou and Yoon, 2011), fluorescent (Chen et al., 2010; Liu et al., 2009, 2010), electrochemical (Granot et al., 2008; Kang et al., 2010), quartz crystal microbalance (QCM) (Luo et al., 2010; Speight and Cooper, 2012) and SPR (Arnell et al., 2006; Sandblad et al., 2009) sensor for chiral discrimination. Lately, the first LSPR based biosensor for chiral analysis has also been reported by our group (Guo et al., 2012a). It should be noted that, because there is no separation steps, highly enantioselective receptors must be used for the fabrication of the enantioselective sensors in order to distinguish the individual response contributions of the enantiomers (Arnell et al., 2006; Sandblad et al., 2009). However, till present only few selectors are found to be highly enantioselective, which seriously limited the widespread development of enantioselective sensors.

Herein, we demonstrate a biosensor employing weak enantioselective and nonselective receptors for chiral discrimination of racemic mixture of TNA. TNA is an import drug intermediate for a number of clinical drugs such as the antidepressant drug sertraline and the negative gating modulators NS8593 (Crewe et al., 1992; Diness et al., 2011; Flament et al., 1999; Jenkins et al., 2011; Koe et al., 1983; Strobaek et al., 2006). The sensor was made up with a dual-channel microfluidic chip. A dense self-assembled gold nanorod (AuNR) monolayer was modified on the inner wall of both channels to act as the LSPR transducers. AuNRs in one channel of the chip was then modified with HSA, and AuNRs in the other channel was modified with anti-TNA antibody. Our investigation showed that the binding affinity of (*S*)-TNA is stronger than (*R*)-TNA on the HSA modified AuNRs, while it is equal on the anti-TNA antibody modified AuNRs. The combinations of LSPR responses collected from the two channels can be used for accurate translating the concentration of (*R*)- and (*S*)-TNA in solution.

2. Experimental section

2.1. Materials

Human serum albumin (HSA), $SH(CH_2)_2(OCH_2CH_2)_7O(CH_2)_2COOH$ (PEG thiol acid), 1-ethyl-3-(3-dimethylaminopropyl)-carbodiimide (EDC), N-Hydroxysuccinimide (NHS), polystyrenesulfonate (PSS), hexadecyltrimethylammonium bromide (CTAB), sodium Borohydride ($NaBH_4$), sodium citrate, gold(III) chloride trihydrate (99.9%), silver nitrate and ascorbic acid were purchased from Sigma-Aldrich Pte. Ltd. Monoclonal anti-TNA antibody was obtained from Zoonbio Biotechnology Co., Ltd. Sodium chloride (NaCl) and aminopropyltriethoxysilane (APTES) were purchased from Merck Chemicals. (*R*)- and (*S*)-TNA were obtained from Alfa Aesar. All the chemicals were used as received.

2.2. Experimental setup

A microfluidic LSPR detection system reported previously (Guo et al., 2012a) was used for the LSPR measurement. Briefly, a portable UV–vis spectrophotometer (Maya2000 Pro) coupled with a Hamamatsu S11510 detector was purchased from Ocean Optics (Dunedin, Florida, USA). A tungsten halogen light source (LS-1) was used for the generation of the LSPR, and two optical fiber bundles (P400-2-VIS-NIR) were used for optical transmission. The spectral resolution of this system is 0.1 nm (FWHM) with a signal-to-noise ratio of 450:1. The LSPR measurements were performed in a transmission mode by the UV–vis spectrophotometer in a wavelength range of 480–880 nm for whole-profile spectral capture, and a wavelength range from 700–780 nm was set for high-resolution spectral capture. All the spectra are measured at room temperature. The exposure time of the CCD camera is set at 1 s for all the experiments.

A glass microfluidic chip with two straight channels (depth × width = 100 × 205 μm) purchased from the Dolomite Centre Ltd (Part no. 3200008) was used for sample detection. Solution was driven into the microfluidic chip with a WZS-50F6 microinfusion system (Medical Instrument Corporation of Zhejiang University, Zhejiang, China). A flow rate of 15 μL/min was set up for all experiments.

2.3. Immobilization of AuNRs

A seed-mediated growth procedure reported previously (Ming et al., 2009; Nikoobakht and El-Sayed, 2003) were utilized for the synthesis of AuNRs. Shortly before the immobilization, the as-synthesized AuNR solution was centrifuged at 6500 rpm for 15 min for two times to remove excess CTAB. The precipitate was then redispersed in 80 mM NaCl solution.

A previously developed method (Ferhan et al., 2010) was used for the immobilization of AuNRs onto the inner wall of the microfluidic chip. Briefly, the modification can be divided into five steps as follow: (i) The microfluidic channels were firstly modified with a self-assembled monolayer of APTES via a method reported earlier (Guo et al., 2010). (ii) 20 mg/mL PSS aqueous solution was injected into the chip and incubated for 1 h. (iii) The channels were rinsed with water, and blown dry with nitrogen. (iv) The CTAB free AuNR solution (in 80 mM NaCl) was injected into the chip and incubated for 5 h. The solution was then replaced with a freshly prepared AuNR solution, and incubated for the other 5 h. The modification procedures were repeated for a third time to ensure the fabrication of a dense monolayer of AuNRs on the chip surface. (v) Finally, the microfluidic channels were rinsed with water and phosphate buffer (0.1 M, pH 7.4) to remove the unbounded AuNRs.

2.4. Surface modification

Protein (HSA and TNA antibody) was immobilized onto the AuNR surface as follow: First, a self-assembled monolayer (SAM) of PEG thiol acid was formed on the AuNR surface by the injection of 5.0 mg/mL PEG thiol acid ethanol solution into the microfluidic channel and incubating for 12 h. Next, a standard amine-coupling procedure was used to establish linkage between the PEG thiol acid and the protein. Briefly, a mixed solution of 0.1 M EDC and 0.05 M NHS was injected into the channel and incubated for 1 h to activate the carboxyl group. Then, a solution containing 0.1 mg/mL protein (HSA or anti-TNA antibody) was injected into the microfluidic channel and incubated for another 2 h to allow the amine-coupling process.

2.5. TNA measurement

TNA binding events were real-time monitored by the LSPR peak shifts ($\Delta\lambda$) of protein modified AuNRs before and after analytes binding. A concentration range from 0–1000 μM was investigated to establish the calibration curves. Single component (*R*)- and (*S*)-TNA binding events obtained from the HSA modified microfluidic channel were used for the construction of single-component enantioselective calibration curves; while the binding events of TNA racemic mixtures obtained from the anti-TNA antibody modified microfluidic channel was used for the construction of nonselective calibration curve. The proposed biosensor was used

for the analysis of standard mixtures of (*R*)- and (*S*)-TNA, and the found values were compared with the added values to evaluate the accuracy of the sensor.

3. Results and discussion

3.1. Principle of the sensor

Enantioselective sensors fabricated with weak chiral selectors cannot distinguish the individual response contributions from the mixture of enantiomers (Arnell et al., 2006). Consequently, those sensors fabricated with weak chiral selectors cannot be used for the assay of racemic mixtures of enantiomers. Herein we propose the use of a dual-channel microfluidic chip, which employs two different kinds of selectors to accomplish the chiral discrimination (Scheme 1). One channel of the chip is modified with non-enantioselective receptors. Both (*R*)- and (*S*)-TNA have the same binding constant in this flow channel; the other channel of the chip is modified with weak enantioselective receptors. It can be presumed that there are two different types of adsorption sites on this kind of receptors, one is enantioselective and the other is nonselective. Both (*R*)- and (*S*)-TNA have the same probability when binding to the nonselective sites. However, only (*S*)-TNA can bind to the enantioselective sites. As a consequent, more (*S*)-TNA would bind to the enantioselective receptors.

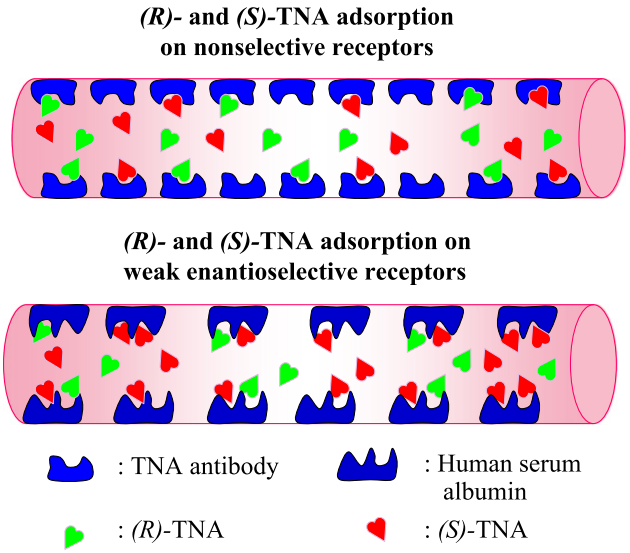

Scheme 1. Schematic diagram of the mechanism of the proposed enantioselective biosensor

At constant temperature, the concentrations of an analyte adsorption on a surface and in the solution at equilibrium can be evaluated by the classical Langmuir isotherm equation:

$$\theta = \frac{q^*}{q_s} = \frac{bC}{1+bC} \tag{1}$$

where θ is the fraction of monolayer coverage of the surface, q^* is the stationary phase concentration at equilibrium with the mobile phase concentration C, q_s is the specific saturation capacity of the stationary phase, and b is a numerical coefficient.

In the present work, the LSPR response is measured in peak wavelength shift ($\Delta\lambda$), which is proportional to the analytes concentration. Therefore, the LSPR response of the sensing unit which employing non-enantioselective receptor is given by the following equation:

$$\Delta\lambda^* = \frac{\Delta\lambda_s bC}{1+bC} \tag{2}$$

In this equation, $\Delta\lambda^*$ is the peak wavelength shift at equilibrium with the analytes concentration of C in solution, and $\Delta\lambda_s$ is the maximum peak shift when the surface is saturated with analytes.

As discussed above, there are two different types of adsorption sites on the weak enantioselective receptors. One is enantioselective and the other is nonselective. Therefore, the bi-Langmuir model was proposed to accounting for adsorption on these heterogenous surfaces (Fornstedt et al., 1999; Fornstedt et al., 1997):

$$\Delta\lambda^* = \Delta\lambda^*_1 + \Delta\lambda^*_2 = \frac{\Delta\lambda_{s,1} b_1 C}{1+b_1 C} + \frac{\Delta\lambda_{s,2} b_2 C}{1+b_2 C} \tag{3}$$

where $\Delta\lambda^*_1$ and $\Delta\lambda^*_2$ are the wavelength shift at equilibrium with the analytes concentration of C in solution contributed by the enantioselective and nonselective adsorption sites, respectively. $\Delta\lambda_{s,1}$ and $\Delta\lambda_{s,2}$ are the monolayer capacities of the enantioselective and nonselective adsorption sites, respectively. The coefficients b_1 and b_2 are related to the adsorption energy on the two types of sites.

3.2. LSPR responses of AuNRs modified with nonselective receptors

The anti-TNA antibody was used as the nonselective receptor for the determination of TNA racemic mixtures. Fig. 1a shows the LSPR spectra of AuNRs modified with anti-TNA antibody before

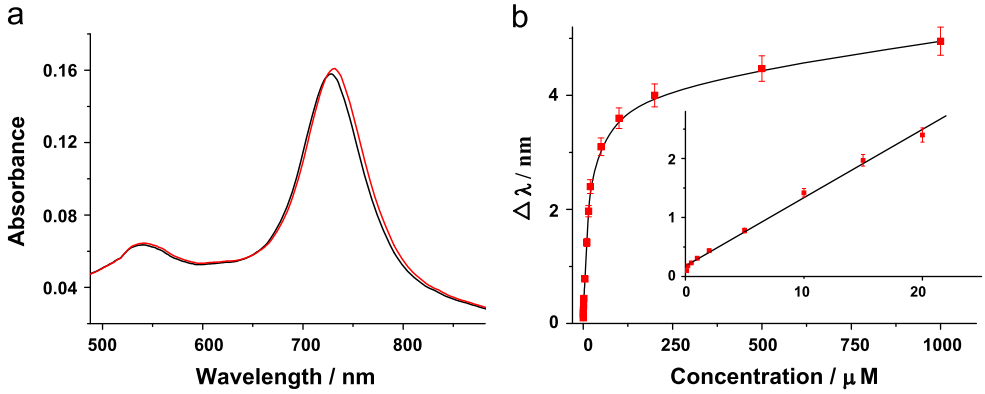

Fig. 1. (a) Typical LSPR spectra of AuNRs modified with anti-TNA antibody before (black) and after (red) the binding of 50 μM TNA. (b) LSPR responses upon binding of racemic mixtures of TNA to the TNA antibody modified AuNRs versus TNA concentration over a concentration range from 0–1000 μM. The inset shows the linear responses of racemic mixture of TNA in low concentration range. Error bars represent standard deviations of three replicates. (For interpretation of the references to color in this figure legend, the reader is referred to the web version of this article.)

(black) and after (blue) TNA binding. After the injection of TNA (50 μM) into the microfluidic chip, significant wavelength shifts were observed at both the transverse and longitudinal peak, indicating the successful binding of TNA onto the AuNR surface. Similar to our previous observations, (Guo et al., 2011a, 2011b) the results showed that the longitudinal peak was much more sensitive than the transverse peak in terms of refractive index change, which was therefore used for quantitative determination of TNA.

Next, we investigated the concentration dependant LSPR peak shifts (Fig. 1b) upon TNA binding. The LSPR responses were increased rapidly with the increasing of TNA (racemic mixture) concentration. Good linear responses were observed in the low concentration range (below 20 μM), as shown in the inset of Fig. 1b and Table 1. The experimental determined limit of detection was 20 nM, with a signal to noise ratio of 4.2.

The single-component concentration dependent LSPR responses for (*R*)- and (*S*)-TNA were investigated (Fig. S1). The two curves were well overlapped with the one obtained from the TNA racemic mixture. These results proved that the anti-TNA antibody used herein was nonselective for the enantiomers. Therefore, this assay can only be used for the determination of the total amount of TNA in solution.

3.3. LSPR responses of AuNRs modified with enantioselective receptors

HSA is reported to be a weak chiral selector for TNA (Su et al., 2009). Therefore, herein HSA was utilized to modify AuNRs on one channel of the microfluidic chip to realize the chiral discrimination of TNA. Fig. 2a shows the LSPR spectra of HSA modified AuNRs before and after the binding of (*R*)- and (*S*)-TNA (50 μM, respectively). Upon the binding of (*R*)-TNA (the blue line), 2.6 nm peak shift was observed; while the binding of (*S*)-TNA with the same concentration (the red line) generated a peak shift of 3.8 nm, which was 1.2 nm greater than the binding of (*R*)–TNA. The enantioseparation efficiency of the sensor can be described by the chiral discrimination factor (α), which is defined as the ratios of the (*S*)- to (*R*)-signals:

$$\alpha = \frac{\Delta\lambda_S}{\Delta\lambda_R} \tag{4}$$

Based on Eq. (4), the chiral discrimination factor of the HSA modified LSPR sensor for (*R*)- and (*S*)-TNA was calculated to be ~1.5.

The LSPR responses of (*R*)-, (*S*)- and racemic mixture of TNA on this sensor were investigated in detail, and the results were shown in Fig. 2b. The peak wavelength shift of all the three components were increased with the increasing of analytes concentration. Similar to Fig. 1 which employs anti-TNA antibody as the receptor, good linear responses were observed in the low concentration ranges, as shown in the inset of Fig. 2b. The linear range was up to 50 μM for both (*R*)- and (*S*)-TNA (see Table 1). The experimental determined single component limits of detection were 150 nM for (*R*)-TNA and 100 nM for (*S*)-TNA.

Interestingly, our investigation revealed that the LSPR responses of the racemic mixture of TNA were equal to the sum of the individual LSPR responses of (*R*)- and (*S*)-components, that is,

$$\Delta\lambda_{mix} = \Delta\lambda_R + \Delta\lambda_S \tag{5}$$

where $\Delta\lambda_R$ is the LSPR response of pure (*R*)-TNA, $\Delta\lambda_S$ is the response of pure (*S*)-TNA, and $\Delta\lambda_{mix}$ is the response of the mixture. A series of experiments were conducted to testify the applicability of this equation in case of enantiomeric excess. First, the LSPR responses of pure (*R*)- and (*S*)-TNA with the concentration range from 0–35 μM were tested; next, the LSPR responses of a series of mixture solutions containing different amount of standard (*R*)- and (*S*)-TNA by controlling the overall TNA concentration at 35 μM were analyzed (Table S1). The results showed that good consistency was achieved between the ($\Delta\lambda_R + \Delta\lambda_R$) and $\Delta\lambda_{mix}$ in all the concentration range investigated herein, which proved the applicability of Eq. (5). However, it should be emphasized that Eq. (5) is only effective in the low concentration, e.g. within the linear response ranges shown in Table 1.

Table 1
Linear equation, linear range and limit of detection.

Target	Linear equation	Linear regression coefficient	Linear range (μM)	LOD (nM)
Racemic mixture[a]	$\Delta\lambda_{ns}$=0.1157C+0.1781	0.9975	0.02–20	20
(*R*)-TNA[b]	$\Delta\lambda_R$=0.048C+0.1758	0.9956	0.15–50	150
(*S*)-TNA[b]	$\Delta\lambda_S$=0.073C+0.3213	0.9952	0.1–50	100

[a] Data obtained from microfluidic channel modified with TNA antibody.
[b] Data obtained from microfluidic channel modified with HSA.

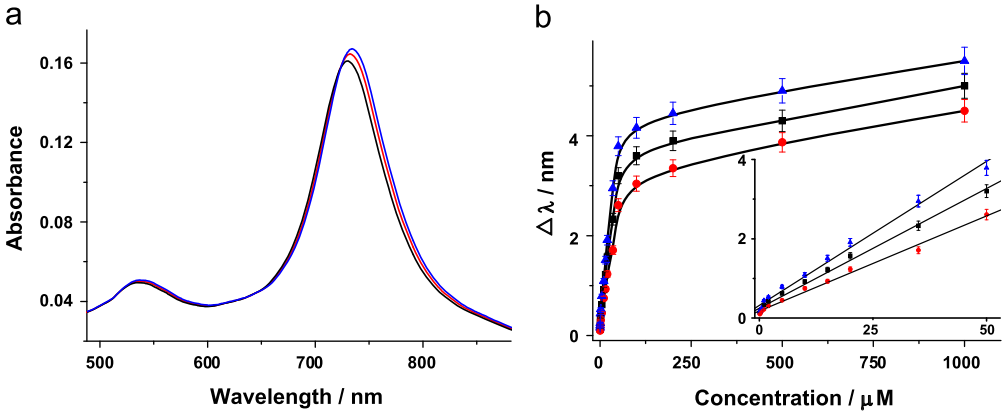

Fig. 2. (a) Typical LSPR spectra of AuNRs modified with HSA before (black line) and after the binding of 50 μM (*R*)—(red line) and (*S*)—TNA (blue line). (b) Binding of TNA to the HSA modified AuNRs versus TNA concentration over a concentration range from 0.1–1000 μM. The main figure shows the LSPR responses of (*R*)—(red dots), (*S*)—(blue triangles) and racemic (black squares) TNA. The inset shows the linear responses of (*R*)—(red dots), (*S*)—(blue triangles) and racemic (black squares) TNA in low concentration range. Error bars represent standard deviations of three replicates. (For interpretation of the references to color in this figure legend, the reader is referred to the web version of this article.)

3.4. Determination of TNA racemic mixtures

Based on Eq. (5) and the linear regression equations shown in Table 1, the individual enantiomer concentration in a TNA racemic mixture can be calculated as follow:

$$\Delta\lambda_{ns} = 0.1157C + 0.1781 = 0.1157(c_R + c_S) + 0.1781 \quad (6)$$

$$\Delta\lambda_{racemic} = \Delta\lambda_R + \Delta\lambda_S = (0.048c_R + 0.1758) + (0.073c_S + 0.3213) \quad (7)$$

The nonselective LSPR response of the mixture ($\Delta\lambda_{ns}$) can be experimentally obtained from the TNA–antibody modified flow channel; similarly, the enantioselective LSPR response ($\Delta\lambda_{racemic}$) can be experimentally achieved from the HSA modified flow channel. Therefore, the individual enantiomer concentration (c_R and c_S) can be calculated by the equation set of Eqs. (6) and (7).

Fig. 3a shows the UV–vis spectra of the microfluidic chips before and after the injection of a standard mixture solution of (*R*)-TNA (5.0 μM) and (*S*)-TNA (10.0 μM). After the injection of the mixture solution, a peak shit of 1.92 nm was observed from the antibody modified channel, while it was 1.47 nm for the HSA modified channel. According to Eqs. (6) and (7), the concentration of (*R*)-TNA was calculated to be 5.24 μM, and the (*S*)-TNA was 9.82 μM. The concentrations of the two isomers calculated from Eqs. (6) and (7) were highly consistent with the concentration added to the solution. The results strongly indicated the applicability of the proposed approach for chiral discrimination of TNA.

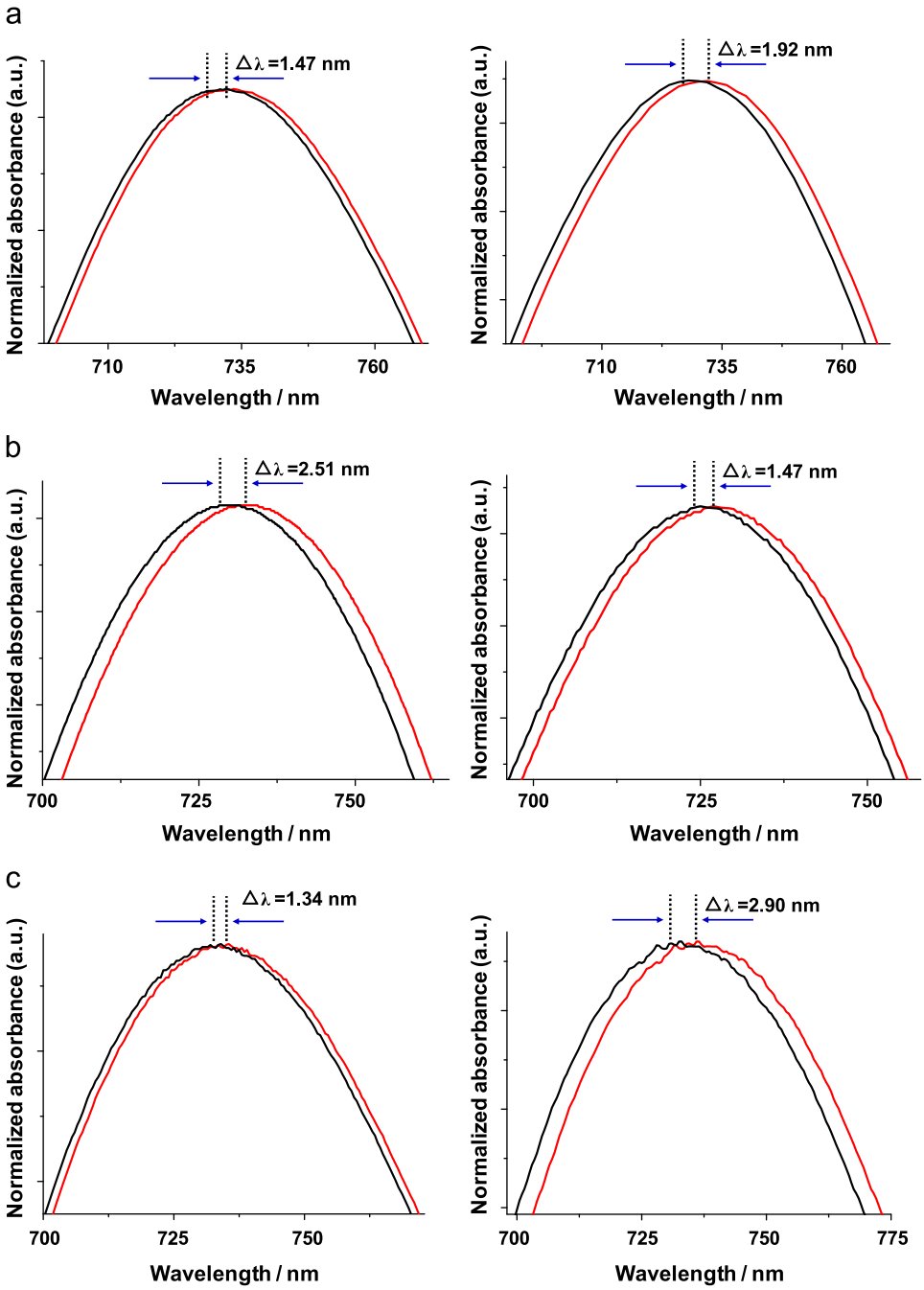

Fig. 3. Typical LSPR spectra of AuNRs modified with TNA antibody (left) and HSA (right) before (black line) and after (red line) the binding of a standard mixture solution containing different amount of TNA: a. 5.0 μM (*R*)–TNA and 10.0 μM (*S*)–TNA; b. 20 μM (*R*)–TNA and 0.15 μM (*S*)–TNA; c. 50 μM (*R*)–TNA and 0.1 μM (*S*)–TNA. Five times dilution was conducted before injection the standard solution of (c) to the TNA antibody modified microfluidic channel. (For interpretation of the references to color in this figure legend, the reader is referred to the web version of this article.)

Table 2
Accuracy of the proposed biosensor for the detection of racemic mixture of TNA*

Added		Found		Relative error (%)	
(*R*)-	(*S*)-	(*R*)-	(*S*)-	(*R*)-	(*S*)-
0.50	0.5	0.48 ± 0.04	0.51 ± 0.03	4.0	2.0
0.20	15	0.20 ± 0.03	15.38 ± 0.58	0	2.5
0.15	20	0.16 ± 0.02	19.84 ± 0.77	6.7	0.8
5.0	10	5.24 ± 0.35	9.82 ± 0.46	4.8	1.8
10	5	10.47 ± 0.47	5.19 ± 0.33	4.7	3.8
15	0.2	14.28 ± 0.52	0.19 ± 0.03	4.8	5.0
20	0.15	20.55 ± 0.86	0.14 ± 0.01	2.7	6.7

* Data represent the average of 5 replicates.

The accuracy of the approach for the determination of individual enantiomer concentration in TNA racemic mixtures was demonstrated by the analysis of a series of standard mixture solutions of (*R*)- and (*S*)-TNA (Table 2). The results showed that the approach can accurately distinguish 0.15 μM (*S*)-TNA/(*R*)-TNA out from 20 μM (*R*)-TNA/(*S*)-TNA. The typical spectra of distinguishing 0.15 μM (*S*)-TNA out from 20 μM (*S*)-TNA were demonstrated in Fig. 3b. In order to show the feasibility of the approach to distinguish (*R*)- and (*S*)-TNA in case of high enantiomeric excess, we also investigated the analysis of a standard solution containing 50 μM (*R*)-TNA and 0.1 μM (*S*)-TNA (500 times enantiomeric excess), and the results were shown in Fig. 3c. It is worth to note that in this case the total concentration of (*R*)- and (*S*)-TNA is not located in the linear range of the TNA-antibody modified channel. Therefore, 5 times dilution was conducted before injection the standard solution to the TNA antibody modified microfluidic channel. These results strongly indicated that the proposed sensor was effective for the chiral discrimination of TNA enantiomers.

4. Conclusions

In this contribution, we demonstrated an approach for accurately chiral discrimination of racemic mixture of TNA by the construction of an LSPR biosensor. The sensor was made up with a dual-channel microfluidic chip. One channel of the chip was modified with a weak chiral selector for (*R*)- and (*S*)-TNA (HSA); the other channel was modified with nonselective binders (anti-TNA antibody). The combination of LSPR responses from the two channels could be used for accurately discrimination of individual (*R*)- and (*S*)-TNA from a racemic mixture solution. The results showed that 0.15 μM (*S*)-TNA/(*R*)-TNA can be accurately distinguished out from 20 μM (*R*)-TNA/(*S*)-TNA, and the relative errors were below 7%. This is the first demonstration of using weak enantioselective and nonselective receptors to construct enantioselective biosensors. It could effectively expend the applicable receptors for enantioselective sensors since most of the previous sensors require the use of highly enantioselective receptors.

Acknowledgments

The authors gratefully acknowledge the financial support of the 973 Program of China (2010CB732403), National Key Technologies R&D Program of China during the 12th Five-Year Plan Period (2012BAD29B06), National Natural Science Foundation of China (21277025, 21205017, 21275031, and 21205016), National Science Foundation of Fujian Province (2012J01036), and the Foundation of Fujian Educational Committee (JA12039).

Appendix A. Supporting information

Supplementary data associated with this article can be found in the online version at http://dx.doi.org/10.1016/j.bios.2013.03.009.

References

Arnell, R., Ferraz, N., Fornstedt, T., 2006. Analytical Chemistry 78 (5), 1682–1689.
Bako, P., Keglevich, G., Rapi, Z., Toke, L., 2012. Current Organic Chemistry 16 (3), 297–304.
Chen, X., Huang, Z., Chen, S.Y., Li, K., Yu, X.Q., Pu, L., 2010. Journal of the American Chemical Society 132 (21), 7297–7299.
Cho, E.N.R., Li, Y., Kim, H.J., Hyun, M.H., 2011. Chirality 23 (4), 349–353.
Crewe, H., Lennard, M., Tucker, G., Woods, F., Haddock, R., 1992. British Journal of Clinical Pharmacology 34 (3), 262–265.
Diness, J.G., Skibsbye, L., Jespersen, T., Bartels, E.D., Sørensen, U.S., Hansen, R.S., Grunnet, M., 2011. Hypertension 57 (6), 1129–1135.
Ema, T., Hamada, K., Sugita, K., Nagata, Y., Sakai, T., Ohnishi, A., 2010. The Journal of Organic Chemistry 75 (13), 4492–4500.
Ferhan, A.R., Guo, L., Kim, D.H., 2010. Langmuir 26 (14), 12433–12442.
Flament, M.F., Lane, R., Zhu, R., Ying, Z., 1999. International Clinical Psychopharmacology 14 (5), 259–276.
Fornstedt, T., Götmar, G., Andersson, M., Guiochon, G., 1999. Journal of the American Chemical Society 121 (6), 1164–1174.
Fornstedt, T., Sajonz, P., Guiochon, G., 1997. Journal of the American Chemical Society 119 (6), 1254–1264.
Granot, E., Tel-Vered, R., Lioubashevski, O., Willner, I, 2008. Advanced Functional Materials 18 (3), 478–484.
Guo, L., Chen, G., Kim, D.H., 2010. Analytical Chemistry 82, 5147–5153.
Guo, L., Ferhan, A.R., LEE, K., Kim, D.H., 2011a. Analytical Chemistry 83 (7), 2605–2612.
Guo, L., Huang, Y., Kikutani, Y., Tanaka, Y., Kitamori, T., Kim, D.H., 2011b. Lab on a Chip 11, 3299–3304.
Guo, L., Yin, Y., Huang, R., Qiu, B., Lin, Z., Yang, H.H., Li, J., Chen, G., 2012a. Lab on a Chip 12 (20), 3901–3906.
Guo, X., Liu, T., Deng, Z., Cane, D.E., 2012b. Biochemistry 51, 879–887.
Hirose, K., Miura, S., Senda, Y., Tobe, Y., 2012. Chemical Communications 48, 6052–6054.
Huang, L., Chen, G., 2011. Analytical Methods 3 (3), 488–508.
Huang, L., Lin, J., Xu, L., Chen, G., 2007. Electrophoresis 28 (15), 2758–2764.
Huang, L., Lin, J.M., Yu, L., Xu, L., Chen, G., 2008. Electrophoresis 29 (17), 3588–3594.
Huang, L., Lin, J.M., Yu, L., Xu, L., Chen, G., 2009. Electrophoresis 30 (6), 1030–1036.
Ikai, T., Okamoto, Y., 2009. Chemical Reviews 109 (11), 6077–6101.
Izake, E.L., 2007. Journal of Pharmaceutical Sciences 96 (7), 1659–1676.
Jenkins, D.P., Strøbæk, D., Hougaard, C., Jensen, M.L., Hummel, R., Sørensen, U.S., Christophersen, P., Wulff, H., 2011. Molecular Pharmacology 79 (6), 899–909.
Kang, Y.J., Oh, J.W., Kim, Y.R., Kim, J.S., Kim, H., 2010. Chemical Communications 46 (31), 5665–5667.
Koe, B.K., Weissman, A., Welch, W.M., Browne, R.G., 1983. Journal of Pharmacology and Experimental Therapeutics 226 (3), 686–700.
Lin, Z., Zhang, J., Cui, H., Zhang, L., Chen, G., 2010. Journal of Separation Science 33 (23–24), 3717–3725.
Liu, H.L., Hou, X.L., Pu, L., 2009. Angewandte Chemie International Edition 48 (2), 382–385.
Liu, H.L., Peng, Q., Wu, Y.D., Chen, D., Hou, X.L., Sabat, M., Pu, L., 2010. Angewandte Chemie International Edition 49 (3), 602–606.
Lu, M., Zhang, L., Qiu, B., Feng, Q., Xia, S., Chen, G., 2008. Journal of Chromatography A 1193 (1–2), 156–163.
Luo, M.L., Zhang, W.G., Zhang, S., Fan, J., Su, W.C., Yin, X., 2010. Chirality 22 (4), 411–415.
Ming, T., Zhao, L., Yang, Z., Chen, H., Sun, L., Wang, J., Yan, C., 2009. Nano Letters 9 (11), 3896–3903.
Nikoobakht, B., El-Sayed, M.A., 2003. Chemistry of Materials 15 (10), 1957–1962.
Nojavan, S., Fakhari, A.R., 2011. Electrophoresis 32 (6-7), 764–771.
Płotka, J.M., Morrison, C., Biziuk, M., 2012. TrAC Trends in Analytical Chemistry 31, 23–37.
Sandblad, P., Arnell, R., Samuelsson, J., Fornstedt, T., 2009. Analytical Chemistry 81 (9), 3551–3559.
Shen, J., Ikai, T., Okamoto, Y., 2010. Journal of Chromatography A 1217 (7), 1041–1047.
Shen, J., Liu, S., Li, P., Shen, X., Okamoto, Y., 2012. Journal of Chromatography A 1246, 137–144.
Sohajda, T., Szakács, Z., Szente, L., Noszál, B., Béni, S., 2012. Electrophoresis 33 (9–10), 1458–1464.
Song, L.X., Bai, L., 2009. The Journal of Physical Chemistry B 113 (34), 11724–11731.
Speight, R.E., Cooper, M.A., 2012. Journal of Molecular Recognition 25 (9), 451–473.
Stefan-van Staden, R.I., M Nejem, R.F., van Staden, J.Y., Aboul-Enein, H, 2011. Current Pharmaceutical Analysis 7 (4), 253–257.
Strobaek, D., Hougaard, C., Johansen, T.H., SORENSEN, U.S., NIELSEN, E.O., Nielsen, K.S., Taylor, R.D.T., Pedarzani, P., Christophersen, P., 2006. Molecular Pharmacology 70 (5), 1771–1782.

Su, W.C., Zhang, W.G., Zhang, S., Fan, J., Yin, X., Luo, M.L., Ng, S.C., 2009. Biosensors and Bioelectronics 25 (2), 488–492.
Sun, P., Wang, C., Breitbach, Z.S., Zhang, Y., Armstrong, D.W., 2009. Analytical Chemistry 81 (24), 10215–10226.
Tang, M., Zhang, J., Zhuang, S., Liu, W., 2012. TrAC Trends in Analytical Chemistry 39, 180–194.
Ward, T.J., Baker, B.A., 2008. Analytical Chemistry 80 (12), 4363–4372.
Ward, T.J., Ward, K.D., 2012. Analytical Chemistry 84 (2), 626–635.
Wu, L., Vogt, F.G., 2012. Journal of Pharmaceutical and Biomedical Analysis 69, 133–147.
Ye, H., Yu, L., Xu, X., Zheng, C., Lin, W., Liu, X., Chen, G., 2010. Electrophoresis 31 (12), 2049–2054.
Yu, L., Chu, K., Ye, H., Liu, X., Xu, X., Chen, G., 2012. TrAC, Trends in Analytical Chemistry 34, 140–151.
Zhang, M., Ye, B.C., 2011. Analytical Chemistry 83 (5), 1504–1509.
Zhou, J., Dai, Y., Wang, S., Zhu, E., Hai, J., Liu, Y., Tang, J., Tang, W., 2012. RSC Advances 2, 5088–5093.
Zhou, Y., Yoon, J., 2011. Chemical Society Reviews 41 (1), 52–67.